Available online at www.sciencedirect.com
SCIENCE DIRECT®
Journal of Chromatography A, 1058 (2004) 3–19
JOURNAL OF CHROMATOGRAPHY A
www.elsevier.com/locate/chroma

Review

High-field asymmetric waveform ion mobility spectrometry: A new tool for mass spectrometry

Roger Guevremont

Ionalytics Corporation, 1200 Montreal Road, Building M50-IPF, Ottawa, Ont., Canada K1A OR6

Abstract

High-field asymmetric waveform ion mobility spectrometry (FAIMS) is a new technology for ion separation at atmospheric pressure. This review introduces the reader to FAIMS, covering topics ranging from the fundamentals and extraction of physical parameters from the raw data, to applications of FAIMS extending from homeland security to environmental analysis to proteomics. The investigation of FAIMS as an ion pre-processing tool for mass spectrometry is in its infancy, but reports in the literature illustrate that FAIMS separates isobaric ions including diastereoisomers, separates isotopes, reduces background ions by isolating ions of interest, and simplifies spectra of complex mixtures by dividing the mixture into a series of simpler subsets of ions. Applications ranging from quantitative analysis of inorganic and organometallic compounds, to studies of the conformers of intact proteins, have been reported. This review is a launching point for further exploration of FAIMS.

Keywords: High-field asymmetric waveform ion mobility spectrometry; Reviews

Contents

E-mail address: roger.guevremont@ionalytics.com.

0021-9673/$ – see front matter © 2004 Elsevier B.V. All rights reserved.
doi:10.1016/j.chroma.2004.08.119

1. Introduction and history of FAIMS

High-field asymmetric waveform ion mobility spectrometry (FAIMS) is believed to have originated in Russia during the early 1980s [1]. The first report describing FAIMS appeared in the refereed literature in 1993 [2]. The technology was brought to the USA by Mine Safety Appliances Company (MSA), and was investigated as a potential tool for portable field detection of explosives and contraband materials. Several company reports [3] and patents [4,5] describe this work. The MSA project was terminated in July 1999.

In the mid-1990s MSA considered partnerships with vendors of mass spectrometers, and approached MDS-Sciex of Toronto, Canada. The researchers at Sciex requested help from scientists at the National Research Council of Canada (NRC) to evaluate the technology that MSA was calling field ion spectrometry (FIS). In collaboration with MSA, the group at NRC developed an interface between the FIS instrument and a Sciex mass spectrometer and published their findings in 1998 [6,7]. The name FAIMS was adopted, to avoid confusion with existing mass spectrometry technology called field ionization mass spectrometry.

The cylindrical geometry version of FAIMS technology embodies a unique capability of focusing ions at atmospheric pressure. Cylindrical geometry was first used in the MSA instrument called FIS, described in a 1995 patent by Carnahan et al. [4]. As a result of a collaboration between MSA and NRC, the concept of focusing in cylindrical geometry was introduced in a 1998 paper in Review of Scientific Instruments [7], and was described in detail [8] the following year, using the first experimental data to confirm the results of ion trajectory calculations. A theoretical description of the ion focusing properties of FAIMS was published by Krylov early in 1999 [9]. The ideas of ion focusing were extended to atmospheric ion trapping, and this technology was experimentally demonstrated later in 1999 [10].

In 1998, a group of researchers located at the Charles Stark Draper Laboratory Inc. (Cambridge, MA) began considering FAIMS as a tool for portable chemical detection. A collaboration with workers at New Mexico State University, including one of the original Russians involved with the development of FAIMS, E.G. Nazarov, resulted in development of a micromachined (MEMS) version of parallel plate FAIMS [11,12].

As a result of the research efforts in Canada, and in Cambridge MA, two spin-off companies were simultaneously formed in late 2001. A Canadian spin-off from the National Research Council of Canada, called Ionalytics Corporation, was formed to exploit FAIMS as an accessory for mass spectrometry. The American counterpart, Sionex Corporation (Waltham, MA), was founded to commercialize a micromachined (MEMS) version of FAIMS called microDMx technology. Ionalytics introduced a FAIMS accessory for mass spectrometry at Pittcon in 2003 in Orlando. Sionex introduced a FAIMS accessory for a Varian portable gas chromatography system at Pittcon 2004 in Chicago.

In this review, the term “FAIMS” will be used exclusively. The technology has been called field ion spectrometer (FIS) [4], ion drift non-linearity spectrometer [13], ion mobility increment spectrometer [14], radio frequency ion mobility spectrometer [15,16] and more recently, differential mobility spectrometer [17,18].

2. The fundamentals of FAIMS

2.1. Flat plate FAIMS

In FAIMS, ions are driven through a bath gas by electric fields, a feature that it shares with conventional drift tube ion mobility spectrometry (DTIMS) [19]. However, in many ways FAIMS is significantly different from DTIMS. Taking an analogy from mass spectrometry, FAIMS resembles a quadrupole analyzer, whereas DTIMS is a time-of-flight analyzer. In a FAIMS device, the ions are separated while they are carried by a flow of gas between closely spaced electrodes, whereas in DTIMS a discreet pulse of ions drifts from an inlet gate to a collector electrode. The ions pass through FAIMS in a continuous stream whereas the ions separated by DTIMS are detected as discrete pulses of ion current as they collide with the collector electrode.

In a FAIMS device, ions are exposed alternately to strong and weak electric fields acting in a direction perpendicular to the flow of carrier gas. These voltages are applied using a high frequency asymmetric waveform [2], characterized by a significant difference in voltage in the positive and negative polarities of the waveform. The separation of ions in FAIMS results from the difference in ion mobility in the strong and weak electric fields. When driven by strong electric fields, the collision between an ion and a molecule of the bath gas is more energetic than thermal energy collisions when the ion is stationary. This change in the energy of collision has subtle effects on the ion mobility [20], in some cases increasing and in some cases decreasing the mobility relative to the mobility at the limit of low field. The change in mobility is a combined result of the properties of both the ion and the bath gas; the mobility of an ion may increase in a one bath gas yet decrease in another. The mobility behavior of many small ions in various gases in strong electric fields has been tabulated [21–24].

A flat plate version of FAIMS was described by Burakov et al. in 1993 [2]. Fig. 1 illustrates the motion of an ion whose mobility is higher in a strong field than in a weak field. The strong field is provided by the application of the peak voltage of the asymmetric waveform which is called the dispersion voltage (DV) and the weak field (of opposite polarity) is applied for a correspondingly longer time. The time–voltage integral for the portion of the waveform in each polarity is equal. After one cycle of the asymmetric waveform shown in Fig. 1, the ion has not returned to its original distance relative to the upper plate, because in this example, the ion mobility in

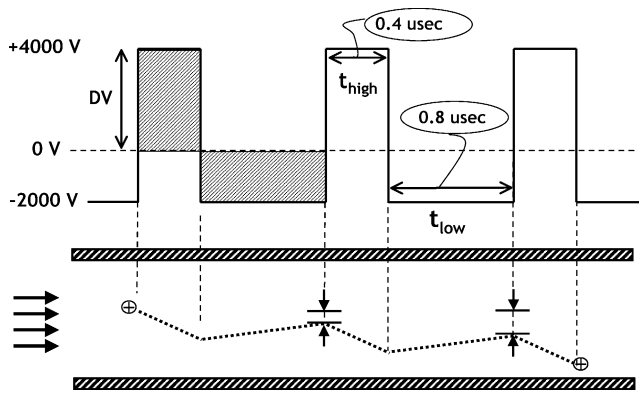

Fig. 1. Ion motion between FAIMS electrodes for an ion having a mobility that increases with electric field strength. The electrodes are about 2 mm apart, and an asymmetric square waveform is applied to the upper electrode. The voltage–time product, shown as shaded areas on the positive and negative portions of the waveform, are equal. The rate of drift towards the lower electrode is greatly exaggerated for illustrative purposes.

the high field was slightly augmented relative to the mobility of the ion in a lower electric field. After a number of cycles of the asymmetric waveform, the ion will collide with the lower electrode. An ion can be successfully transported between the electrodes if a weak electric field is superimposed to compensate for its drift, and thus the ion of interest can be prevented from colliding with the wall. This weak field originates from a dc compensation voltage (CV) applied between the pair of electrodes.

The waveform shape illustrated in Fig. 1 is not used in practice because of very high electrical power requirements (and potential safety concerns). The waveform shape used by the Guevremont group [7] and MSA [4,5] is a combination of a sine wave and its harmonic described by:

$$V(t) = (2/3)D\,sin(\omega t) + (1/3)D\,sin(2\theta\omega t - \Phi) \quad (1)$$

where D is the peak voltage on the high voltage portion of the waveform (DV), ω the waveform frequency in radians/s and Φ a phase shift of $\pi/2$ radians. Energy consumption (and safety concern) is minimized by using inductor–capacitor (LC) tuned electronic circuits.

Eiceman and collaborators who work with the micromachined version of FAIMS use a waveform generator based on a flyback transformer design [25] originating in Russia [26]. The waveform shape is shown in recent publications from Eiceman et al. [27], and by Buryakov [28].

The shape of the waveform is one of several parameters contributing to the value of experimentally measured CV for transmission of an ion through FAIMS. A symmetrical waveform (including a sinusoidal wave) should result in CV = 0 V for transmission of all types of ions. At the other extreme, a very high asymmetry also results in low CV because the distance the ion travels under conditions of high field approaches zero when the time of the applied high voltage becomes short[29]. Eiceman et al. [27] processed the actual waveform used in their experiments using numerical procedures to produce the 'form factors' describing the waveform. Buryakov [30] also reported a set of coefficients unique to their waveform generator. Viehland et al. [31] were able to calculate exact results using the waveform described by Eq. (1). Because the shape of the waveform is critical to the experimentally measured CV, data about specific compounds cannot be used (or compared) by other researchers if the report lacks specific details about the waveform. Several early reports lack specifics about the shape of the waveform.

2.2. Cylindrical geometry FAIMS: ion focusing and trapping

A cylindrical design of FAIMS electrodes was first described by researchers at MSA [4]. This approach was adopted by Guevremont et al. [6] in collaboration with MSA, and the FAIMS was interfaced to a PE-Sciex mass spectrometer. The apparently anomalous increase of sensitivity with increasing applied asymmetric waveform voltage, and the behavior of the device with the change of polarity of the waveform, led to the conclusion that the device was focusing ions [6,7]. This hypothesis was confirmed experimentally soon afterwards [8]. A theoretical discussion of focusing was presented by Krylov [9] in the same year. A typical cylindrical FAIMS electrode system used for ESI–FAIMS–MS is shown in Fig. 2. The inner electrode is a cylinder with a hemispherical tip. The asymmetric waveform, and the dc compensation voltage are applied to the inner electrode. The FAIMS is mounted gas-tight against the orifice plate of the mass spectrometer.

The focusing of ions at atmospheric pressure was utilized to build a FAIMS device for trapping ions [10,32,33]. By selectively gating ions into the FAIMS ion trap, and monitoring the exponential decay of the population of ions in the cloud, the half-lives of various ions in this trap was estimated [33]. Fig. 3 illustrates the decrease in time, of the trapped cloud of ions from two amino acids.

The focusing of ions in cylindrical geometry is also a principle factor contributing to the shape of the peaks obtained

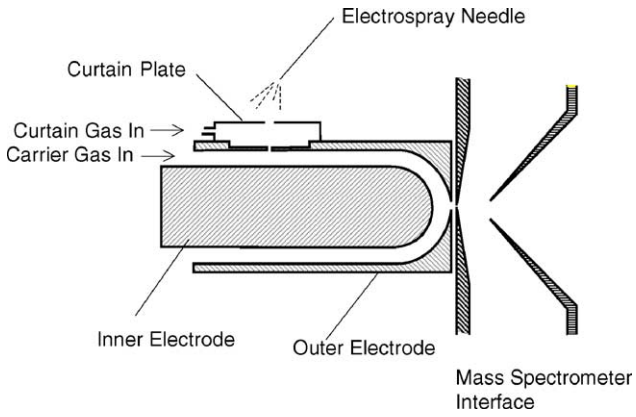

Fig. 2. Cylindrical electrodes used for ESI–FAIMS–MS. The asymmetric waveform and dc compensation voltage are applied to the inner electrode.

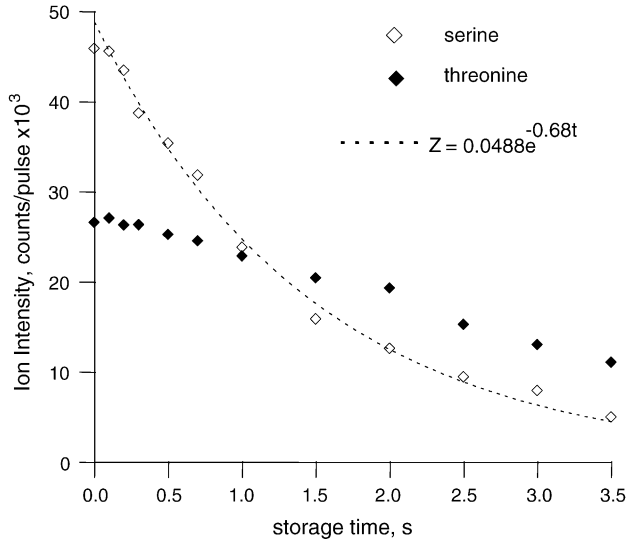

Fig. 3. The decay of a cloud of ions trapped at atmospheric pressure in a FAIMS ion trap [33]. The ions were injected for 900 ms, and the ion trap isolated from the input stream of ions. The exit lens stopping voltage was lowered after a selected storage time, and the residual ion population in the cloud was detected. Half-life of serine ions was about 1 s, whereas the threonine ions were stored more efficiently and their half-life in the trap exceeded 3.5 s.

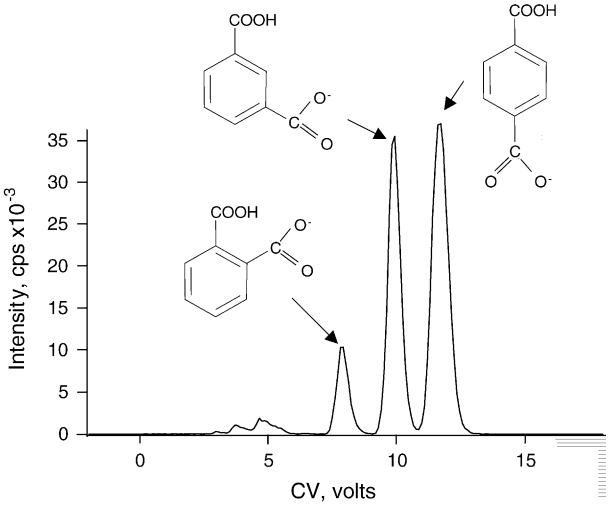

Fig. 4. Scan of the compensation voltage while monitoring *m*/*z* 165 of the *ortho*-, *meta*- and *para*-isomers of phthalic acid.

when sweeping the compensation voltage. The fundamental physics responsible for peak shapes has been described in terms of the confining effects of ion focusing between concentric cylindrical FAIMS electrodes, and the dispersive effects of diffusion and ion–ion repulsion [34,35]. Further details will be presented in Section 2.5.

2.3. Mixtures of gases

Ion mobility at high-field strength is a result of the interaction between the ion and the bath gas. The physical chemistry of this process has been discussed in detail by Mason and McDaniel [20]. The physical chemistry of interaction between ions and carrier gases used in FAIMS (N_2, O_2, CO_2, NO_2 and SF_6) was considered in a collaborative report between Guevremont et al. and Viehland [36]. The long range ion-induced dipole attractive force between the ion and bath gas establishes a potential well whose depth is a function of the polarizability of the bath gas molecule and the size and charge of the ion. The impact of this potential well on ion mobility is dependent on the depth of the well in relation to the thermal energy available at the temperature of the bath gas. The mobility of an ion increases with E/N (where E is the electric field and N is the number density of the bath gas) if the well is deep relative to thermal energy. This is a result of additional energy made available through collisions with the bath gas, thus reducing the effective depth of the potential well. For ion-bath gas combinations in which the thermal energy is comparable or exceeds the well depth, the ion mobility increases less rapidly or decreases as a function of E/N [36]. Decreases in ion mobility in strong fields can be attributed to energy lost in interacting collisions. More specifically, the outer electrons of the ion and the bath gas may lead to the formation of new orbitals (see Mason and McDaniel [20], pages 245–246 for discussion of the behavior of Li^+ and H^+ ions in helium).

The mobility of an ion in a mixture of gases can be estimated using Blanc's Law [20,37]. Using FAIMS, it was shown that Blanc's Law is applicable to the phthalic acid anion in gas mixtures of varying mole fractions of nitrogen and oxygen [38]. However, significant deviation from this simple prediction was shown for gas mixtures of N_2 and CO_2. This phenomenon permitted the practical separation of the three positional (*ortho*-, *meta*-, *para*-) isomers of phthalic acid [38]. Fig. 4 illustrates the separation of the isomers of phthalic acid using a mixture of 95% nitrogen and 5% CO_2, monitoring *m*/*z* 165 while scanning the compensation voltage from 0 to 15 V. A mechanism based on the dynamic formation and dissociation of clusters of the ion and CO_2 (or other complexing molecules) during the low field and high-field portions of the asymmetric waveform has been postulated [15,39,40].

Eiceman et al. [40] also observed that 100–10,000 ppm water in the carrier gas had significant effects on the measured compensation voltages of a number of organophosphorus compounds. It was suggested that the ions collide with water molecules during the low-field cycle of the waveform and form complexes of lower mobility, and that these complexes are dissociated during the high-field portion of the waveform. Furthermore, the authors suggest that at a concentration of water below about 50 ppm, it is unlikely that collisions can occur with a water molecule during the low field portion of the waveform. Therefore, they did not observe nor expect to observe an increase in CV originating from the presence of water at low water concentrations. While this is to be expected given the sensitivity to CV of their experimental operating conditions, further work is warranted to determine the effect of low concentrations of water. The authors also

observed that the presence of water had a significant effect on the measured CV of transmission of the protonated ions of the organophosphorus compounds, but had a minimum effect on the protonated dimers of the same compounds. Similarly, the Eiceman group reported addition of compounds to modify the carrier gas in FAIMS for the detection of explosives [18]. The change in behavior of ions in FAIMS by the addition of modifier gases was attributed to the formation and dissociation of complexes between the ion and the chemical modifier that occur in-phase with the asymmetric waveform.

More recently, Shvartsburg et al. [41] described a universal model for the FAIMS separations in mixtures of gases, derived from the physical chemistry fundamentals that determine the high-field mobilities in heteromolecular gases [20]. This report predicts spectacular non-Blanc effects in mixtures of disparate gases such as He/CO_2, and He/SF_6. The basis of this effect is related to the widely differing molecular masses of these gases, and the large difference in the mobility of an ion in each of the pure gases that compose these mixtures. The model predicts results that closely match experimental observations for small ions (including Cs^+) in mixtures that included He/N_2, He/CO_2 and He/SF_6. These results suggest that although the model of complexation and dissociation, in which ions are associated with a component in the gas during the low-field portion of the waveform, followed by dissociation during the high-field portion of the waveform may be valid under some circumstances, significant non-Blanc behavior can occur even in the absence of this type of complexation.

2.4. Measurement of ion mobility at high E/N using FAIMS

The following two sections of this review deal with physical chemistry, and may be skipped by those readers interested in applications of FAIMS for chemical analysis.

This section describes using FAIMS to quantitatively measure the high-field mobility of an ionized compound. This measurement is not required for the typical application of FAIMS for chemical analysis, but rather is a physical chemistry measurement that, in the future, may form the basis of creation of libraries of the properties of the ions upon which the FAIMS separation is based. This section and Section 2.5 are provided for reference purposes, so that the interested reader will have access to the widest possible scope of information about FAIMS and can use this review as a launching point for further investigation.

Because the FAIMS device may be fabricated in many ways, and operated over a range of gas pressure conditions, a comparison of data originating in different laboratories requires that researchers report their results in a common format. A comparison of measurements taken for an ion, for example Cs^+, between two laboratories with electrodes spaced apart differently, and at different geographical elevations, can be made only if each laboratory reports their results for the high-field mobility of Cs^+ in a format agreed upon by all. Fortunately, Mason and McDaniel [20] provide an approach that is widely accepted.

The high-field properties of ions have been studied for more than 50 years, and a considerable body of literature describing the physical chemistry of interactions between ions and molecules of a bath gas is available [20–24]. The change in mobility with electric field strength was generally described as a polynomial function [20] of the even terms of the ratio of electric field to number density of the gas (E/N), shown in Eq. (2). For convenience, the value of E/N is reported in townsend (Td) which is 1×10^{17} (E/N) where E is V/cm and N is number density (per cm^3). It is recommended that all data acquired with FAIMS be converted from conventional V/cm to Td. Although obtaining the gas pressure (thus N used for the experiment) is never required for mass spectrometry, in FAIMS experiments, measurement of gas pressure is necessary to ensure that data collected at laboratories at different elevations above sea-level arrive at comparable results. The ion mobility at elevated (E/N) can be described by:

$$K_{\mathrm{mob}}(E/N) = K_{\mathrm{mob}}^{(0)} \frac{N_0}{N} \left\{ 1 + \alpha_2 \left(\frac{E}{N} \right)^2 + \alpha_4 \left(\frac{E}{N} \right)^4 + \cdots \right\} \quad (2)$$

where K_{mob} is the mobility at field strength (E/N), $K_{\mathrm{mob}}{}^{(0)}$ the ion mobility at the low field limit at standard temperature and pressure conditions, N the number density of the bath gas, N_0 the number density at standard conditions, and α_2, α_4, α_6, ... are parameters that describe the behavior of mobility as a function of E/N.

For convenience, the parts of Eq. (2) that depend on E/N can be considered together as the 'alpha function' [27,40] that describes the change in mobility of the ion at elevated E/N.

The alpha function is:

$$\alpha(E/N) = \left\{ \alpha_2 \left(\frac{E}{N} \right)^2 + \alpha_4 \left(\frac{E}{N} \right)^4 + \cdots \right\} \quad (3)$$

Mason and McDaniel [20] warn that such relationships have limited value in describing the high-field behavior of ions and that the values of the α_2, α_4, α_6, ... parameters should be used with caution at high-field strength. The terms α_2, α_4, α_6, ... have no intrinsic physical meaning and only are used to provide a mathematical tool with which to calculate $K_{\mathrm{mob}}(E/N)$, which does have physical meaning. In the past, these intermediate values were discarded and the values of $K_{\mathrm{mob}}(E/N)$ were tabulated [21–24]. Despite the limitations of the alpha function, this approach offers a mechanism for comparison of data collected by different authors using different instrumental systems and collected under different conditions of gas pressure. The alpha function must never be extrapolated to E/N conditions extending beyond the range used to collect the original data.

The application of FAIMS for determining the high-field mobility of ions was demonstrated by Viehland et al. [31]. FAIMS data was used to calculate the high-field mobility of the chloride anion, and results were compared with literature values. Using Eq. (4), the FAIMS data values of compensation voltage (C) and dispersion voltage (D), were converted into the $\alpha_2, \alpha_4, \alpha_6, \ldots$ parameters shown in Eq. (2). Eq. (4) is only applicable for a waveform of the type shown in Eq. (1). For simplicity, the higher order parameters beyond α_2 and α_4 are not included in Eq. (4).

$$-C = \alpha_2 \left(\frac{D^3}{9} + \frac{15CD^2}{18} + C^3 \right) + \alpha_4 \left(\frac{55D^5}{486} + \frac{55CD^4}{72} + \frac{10C^2D^3}{9} + \frac{25C^3D^2}{9} + C^5 \right) \quad (4)$$

where C is the value of the compensation voltage, D value of the dispersion voltage, both in townsend (Td). A tutorial style discussion of the pros/cons/pitfalls of this method of calculation of the high-field behavior of ions can be found on the FAIMS technology web site [42].

Eq. (4) only includes terms for α_2 and α_4. Table 1 summarizes the terms from α_2 to α_{10} for either the waveform described by Eq. (1), or with any other asymmetric waveforms for which the values of $\langle f^x \rangle$ have been calculated. The $\langle f^x \rangle$ is the integrated value of the xth power of the points of one cycle of the waveform. For example, when using Eq. (1), the $\langle f^3 \rangle$ is calculated by taking the cube of each point of the equation and integrating over one cycle of the normalized waveform, and is equal to 0.111 or 1/9.

Column 1 of Table 1 are the terms in Eq. (4) that are multiplied by α_2, column 2 are the terms multiplied by α_4, and so on. For example, when using Eq. (1), $-C = \alpha_2\ (C^3 + 0.833CD^2 + 0.111D^3) + \alpha_4\ (C^5 + \ldots)$ which is equivalent to Eq. (4). When using other waveforms, $-C = \alpha_2\ (C^3 + 3\langle f^2 \rangle CD^2 + \langle f^3 \rangle D^3) + \alpha_4\ (C^5 + 10\langle f^2 \rangle C^3D^2 + 10\langle f^3 \rangle C^2D^3 + \ldots$ which is the most generalized relationship between the experimental values of C and D, the applied waveform and the high-field behavior of an ion. The method for calculation of the parameters in Table 1 was described by Viehland et al. [31].

As noted above, Eq. (4) cannot be applied when FAIMS data is collected using a waveform with a shape differing from that of Eq. (1). For other waveforms, an alternate version of Eq. (4) is produced using the parameters shown in Table 1.

The mathematics described in this section is used to extract high-field mobility parameters from the raw FAIMS data, so that the physical chemistry properties of a compound can be described quantitatively. In the future, libraries of the properties of compounds may be developed, based on these measurements. However, at the present time, for most applications of FAIMS to chemical analysis, calculations of this type are unnecessary. In most applications, the compensation voltage for transmission of a given compound through FAIMS is established experimentally using a known standard of the compound, and the analysis is carried out with FAIMS operating at this compensation voltage.

2.5. Other studies of the fundamentals of FAIMS

Spangler [15] discussed the principles of FAIMS for field portable monitoring applications. In a later paper, Spangler [43] reported that the compensating field used to separate ions in FAIMS is directly proportional to the ion mobility, which he suggested would the allow FAIMS data to be compared with DTIMS data. The separation of ^{35}Cl and ^{37}Cl isotopes using FAIMS [44], the separation of the amino acids leucine and isoleucine [45], and the separation of the *o*-, *m*- and *p*-isomers of xylene [12] and phthalic acid [38] by FAIMS suggest that Spangler's assertion of a proportionality between the compensation field and the ion mobility as measured by DTIMS may not be valid. Spangler [43] also reported that the compensation field is related to the cube of the dispersion field. This observation is consistent with the first term on the RHS of Eq. (4) shown above, but may be overly simplistic. The tables of mobility at elevated E/N appearing in Atomic Data and Nuclear Data Tables [21–24] and plots of the alpha function for various ions [27,40] suggest that the higher order parameters including α_4 and α_6 in Eqs. (2) and (3) cannot be ignored as suggested by Spangler.

Table 1
Parameters for producing Eq. (4) with alpha terms [31] from α_2 to α_{10}

α_2	α_4	α_6	α_8	α_{10}
1.000000 C^3	1.000000 C^5	1.000000 C^7	1.000000 C^9	1.000000 C^{11}
0.833333 $\{3\langle f^2 \rangle\} CD^2$	2.777777 $\{10\langle f^2 \rangle\} C^3D^2$	5.833333 $\{21\langle f^2 \rangle\} C^5D^2$	10.000000 $\{36\langle f^2 \rangle\} C^7D^2$	15.277777 $\{55\langle f^2 \rangle\} C^9D^2$
0.111111 $\{\langle f^3 \rangle\} D^3$	1.111111 $\{10\langle f^3 \rangle\} C^2D^3$	3.888888 $\{35\langle f^3 \rangle\} C^4D^3$	9.333333 $\{84\langle f^3 \rangle\} C^6D^3$	18.333333 $\{165\langle f^3 \rangle\} C^8D^3$
	0.763888 $\{5\langle f^4 \rangle\} CD^4$	5.347222 $\{35\langle f^4 \rangle\} C^3D^4$	19.250000 $\{126\langle f^4 \rangle\} C^5D^4$	50.416667 $\{330\langle f^4 \rangle\} C^7D^4$
	0.113168 $\{\langle f^5 \rangle\} D^5$	2.376543 $\{21\langle f^5 \rangle\} C^2D^5$	14.259259 $\{126\langle f^5 \rangle\} C^4D^5$	52.283950 $\{462\langle f^5 \rangle\} C^6D^5$
		0.807184 $\{7\langle f^6 \rangle\} CD^6$	9.686214 $\{84\langle f^6 \rangle\} C^3D^6$	53.274177 $\{462\langle f^6 \rangle\} C^5D^6$
		0.102023 $\{\langle f^7 \rangle\} D^7$	3.672839 $\{36\langle f^7 \rangle\} C^2D^7$	33.667694 $\{330\langle f^7 \rangle\} C^4D^7$
			0.883777 $\{9\langle f^8 \rangle\} CD^8$	16.202577 $\{165\langle f^8 \rangle\} C^3D^8$
			0.091687 $\{\langle f^9 \rangle\} D^9$	5.042819 $\{55\langle f^9 \rangle\} C^2D^9$
				0.964780 $\{11\langle f^{10} \rangle\} CD^{10}$
				0.083515 $\{\langle f^{11} \rangle\} D^{11}$

When used with the waveform described by Eq. (1), the numeric value in the upper left corner of each cell can be used to replace the term $\{x\langle f^y \rangle\}$. For other waveforms, use the $\{x\langle f^y \rangle\}$ terms calculated for the real waveform, without the numerical value.

In a comparison of the transmission efficiencies of planar and cylindrical FAIMS, Krylov [46] developed a function called the coefficient of ion transmission, defined in terms of the measured compensation voltage, dispersion voltage, dimensions of the analyzer, and the gas flow rate. It was shown that in all cases, the ion transmission through flat plates decreases as the applied asymmetric waveform voltage is increased, and that the loss rate is highest for types of ions with high coefficient of diffusion (and high ion mobility). In all cases, the transmission of ions increases with field strength using coaxial cylindrical geometry FAIMS. Theoretical calculations of the coefficient of ion transmission were reported for ions having high experimental CV's (glycine) versus ions with low CV's (leucine) using results for the alpha function available in the literature [29]. Unfortunately, Krylov applied the alpha function to fields up to 80 Td, well beyond the maximum of 67 Td used to collect the original data, with catastrophic consequences. This illustrates one of the most serious limitations of using the alpha function described by Eq. (2) above, and strongly suggests that simple tabulation of $K_{mob}(E/N)$ may be preferable to reporting the terms in the alpha function.

The focusing of ions in cylindrical geometry is a principal factor contributing to the shape of the peaks in the sweep of compensation voltage. The fundamental physics responsible for the shapes of peaks has been described in terms of the confining effects of ion focusing between concentric cylindrical FAIMS electrodes, and the dispersive effects of diffusion and ion–ion repulsion [34,35]. It was shown that the shape of the cloud of ions in a radial direction could be defined as steady-state balance between the focusing electric field and diffusion to yield the time-independent distribution shown in Eq. (5) [34].

$$n(r) = n_p exp\frac{-KV_v(r)}{D} \quad (5)$$

where $n(r)$ is the radial distribution of the number density of ions, n_p the number density at the peak of the distribution, K the mobility of the ion, $V_v(r)$ the virtual potential well (volts), and D the coefficient of diffusion of the ion. The potential well is calculated using numerical methods to simulate the trajectory of the ions between the concentric cylinders [32]. The trajectory calculation requires the dimensions of the FAIMS electrodes, the dispersion voltage and shape of the asymmetric waveform, the compensation voltage and the high-field behavior of the mobility of the ion. Fig. 5 illustrates a potential well between cylindrical electrodes of radii 0.8 and 1.0 cm. The $V_v(r)$ was calculated using numerical methods and the normalized distribution calculated using Eq. (5) with n_p equal 1.0.

Peak shape in the CV spectrum is a consequence of the location of the bottom of the potential well relative to the electrode walls at a given value of CV, and the distribution of ions around this point, $n(r)$, shown in Fig. 5. By assuming an ion transit time through FAIMS of about 250 ms, the loss of ions to the walls was estimated at each value of CV.

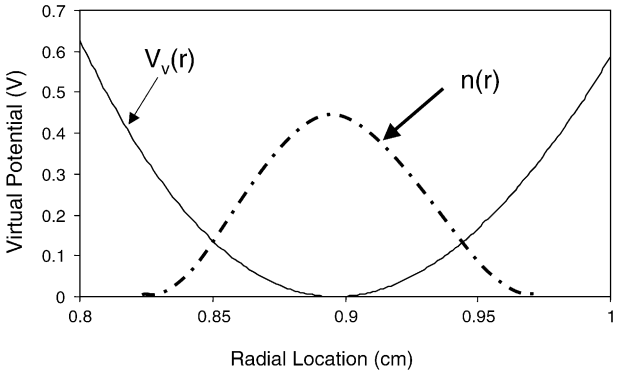

Fig. 5. The virtual potential well ($V_v(r)$) and calculated normalized ion distribution ($n(r)$) between cylindrical electrodes of radii 0.8 and 1.0 cm. The potential well was calculated at DV 3960 V CV −16.5 V, at 298 K, 760 Torr, for an ion with α_2 7.98×10^{-6}, α_4 -3.05×10^{-10} (in Td). The ion distribution was calculated with n_p of 1.0 and ratio of K/D of 39 in Eq. (5).

Guevremont et al. [34] described the loss of the ions to the walls as the overlap of the time-independent equilibrium distribution ($n(r)$ per Eq. (5)) with the electrode wall, leading to a gradual leakage of ions out of the distribution. The distribution shown in Fig. 5 was calculated at CV −16.5 and DV 3960 V. The bottom of the virtual potential well moves radially as a function of CV, and the ion distribution $n(r)$ begins to overlap with the inner electrode at CV −17.6 V and with the outer electrode at −15.5 V. Beyond this voltage range, ion distribution decreases with time through collisions with the electrode walls. The effect of ion–ion space charge repulsion was ignored in these calculations.

Shvartsburg et al. [35] simulated a multitude of ion trajectories that on average describe the behavior of the ion cloud in space and time, and also include ion–ion repulsion within the cloud of ions. Good agreement between calculated and experimental peak shapes were reported by both the Guevremont [34] and the Smith groups [35].

Although operation of the FAIMS technology is based on the change in mobility of an ion in strong electric fields, an approach has been reported that may make it possible to calculate the low field mobility of an ion from FAIMS data [29]. The low field mobility of a number of amino acids was calculated using this approach. Further investigation of this approach is warranted, since it is not apparent by what mechanism the FAIMS data is affected by the low field mobility of the ion.

3. Application to mass spectrometry

3.1. Introduction

When used in conjunction with mass spectrometry, the FAIMS device is used to separate ions prior to their introduction into the vacuum chamber of the mass spectrometer. In practice therefore, the FAIMS is physically located

between an atmospheric pressure ion source and the inlet to the mass spectrometer; one example shown in Fig. 2. The presence of the FAIMS device mounted between an ion source, for example an electrospray ionisation (ESI) needle as shown in Fig. 2, and the ion inlet to the mass spectrometer rarely interferes with existing condensed phase experiments such as liquid chromatography or capillary electrophoresis and should never interfere with the mass spectrometric experiment.

Consider an overview of one example of an LC–FAIMS–MS experiment. A first separation of neutral compounds is carried out in the condensed phase, after which the compounds are ionized by electrospray ionization. The ionic cloud is separated from the HPLC solvent vapor by a counter-current flow of curtain gas (see Fig. 2). This complex mixture of newly formed ions is passed into FAIMS and subjected to a second separation at atmospheric pressure while the stream of ions is being transported through FAIMS by a carrier gas. Finally, the sub-set of the original mixture of ions that is successfully transmitted through FAIMS is delivered to the mass spectrometer for a third separation based on mass-to-charge ratio (*m*/*z*). In some cases, an ion fragmentation step based on collision-induced dissociation (CID) is the equivalent to a fourth dimension of separation. The separation of very complex mixtures is possible, based on these four independent dimensions.

Next, we review a procedure for one type of simple analysis using an LC–FAIMS–MS system. In a first step, a standard solution of a target analyte is delivered by direct infusion to the ionization source, for example an ESI source shown in Fig. 2. Mass spectra are collected during a scan of the CV, and displayed using an approach equivalent to a display of LC–MS data except that the retention time is replaced by CV. A reconstructed chromatogram plot, in this case a CV ionogram of the *m*/*z* of the target analyte ion will reveal the peak compensation voltage suitable for transmission of this ion. This data processing step is exactly analogous to establishing the LC retention time of the target compound. When using an isotopically labeled version of the analyte, it is also recommended that the CV ionogram be checked to ensure that this isotopomer is also transmitted at the same CV as the target analyte. FAIMS is capable of separation of isotopes!

In a second step of this example analysis, the liquid chromatograph is connected to the ionization source and the samples injected in the conventional manner, with the CV set to transmit the analyte ion of interest through FAIMS, and the mass spectrometer set to monitor the *m*/*z* of the ion of interest. A calibration is carried out using a set of standard samples, and where possible including an isotopically-labeled version of the analyte as the internal reference. Quantitative analysis is carried out in the conventional manner, while the CV applied to FAIMS remains unchanged during the entire procedure.

Since FAMS is a relatively rapid separation, the ions spending less that 500 ms inside the FAIMS, a scan of CV usually only requires a few minutes. The value of CV is reproducible, but must be experimentally determined when conditions including DV, gas mixture composition, gas temperature or gas pressure are changed.

In most of the examples discussed below, the FAIMS device is used to conduct a separation which may have otherwise required a liquid chromatograph. The replacement of an LC separation by a FAIMS separation often simplifies the analysis, but may also significantly reduce the time and effort required to develop the LC–MS method. The FAIMS technology is in its infancy, and many investigations will be required to establish the eventual role to be played by FAIMS within the multi-dimensional separations typical of modern chemical analyses.

3.2. Separation and detection of inorganic and organometallic ions

The trace analysis of inorganic ions using traditional electrospray ionization with mass spectrometry has been reported, however the background ion intensity at low *m*/*z* precluded a low detection limit [47]. FAIMS significantly reduces this problem by separating the analyte ions from the background ions. This approach was first used to show the trace detection of chlorate, bromate and iodate using ESI [48]. Detection limits of 3, 13 and 71 ng/L for chlorate, bromate and iodate, in a matrix of 0.2 mM ammonium acetate and 9:1 (v/v) methanol/water were reported. In addition to the reduction of background ion intensity by three to four orders of magnitude relative to conventional ESI, the FAIMS system also separated isobaric ions that interfere with each other in conventional ESI. It was shown that the potential interference of iodide (*m*/*z* 127) on bromate was eliminated because these ions are transmitted through the FAIMS device at different CV values. The potential interference of drinking water disinfection biproducts (DBPs), including dichloroacetate anion (*m*/*z* 127, 129 and 131), with bromate is also avoided by separation with FAIMS.

Significant improvement in the detection of perchlorate was shown using ESI combined with FAIMS–MS [49]. Methods for the quantitative analysis of perchlorate in matrices including drinking water, waste water and urine were developed [50]. Detection limits of perchlorate using ESI–FAIMS–MS were 0.05 ppb in tap water, and 0.37 and 0.50 ppb in waste water and river water respectively. The separation provided by FAIMS completely eliminated the isobaric overlap problem of bisulfate and dihydrogenphosphate on perchlorate.

The application of FAIMS to the chemotherapeutic cancer drug cisplatin, and its hydrolysis products has been reported by Mester et al. [51]. This report illustrates the advantage of FAIMS over conventional inorganic detection approaches, including ICPMS, which measure platinum content but usually cannot differentiate among coexisting species of the platinum-containing drug. Analysis by LC–ESI–MS is feasible, but the detection is limited by the background noise of ESI. In a comparison of LC–ESI–MS and LC–ICPMS for

analysis of platinum drugs, Smith et al. [52] reported a limit of quantitation of the platinum-containing anticancer drug ZD0473 of about 5 ng/mL using LC–ESI–MS/MS and about 0.1 ng/mL using LC–ICPMS. In both cases, the LC run time was 7 min. Using a FAIMS–MS system (without MS/MS). Mester et al. [51] investigated the direct-infusion analysis of cisplatin and its hydrolysis products using mixtures of gases including a ternary mixture of helium, carbon dioxide and nitrogen. The background noise was 30-fold reduced when compared to conventional ESI–MS. Analytical results were linear over 10–200 ng/mL for intact cisplatin with a detection limit of 0.7 ng/mL. No derivatization or chromatographic separation was required.

The Mester group also described the application of FAIMS to the study of water-soluble species of arsenic in marine samples including dogfish muscle, dogfish liver, and lobster hepatopancreas tissues [53]. In particular, FAIMS permitted the identification of arsenocholine and tetramethylarsonium species where conventional ESI–MS was unsuccessful due to high background ion intensity. The low background ion intensity (up to 25-fold lower than ESI–MS) also permitted the application of ESI–FAIMS–MS/MS for confirming structures of some organoarsenic species.

3.3. Separation and detection of small organic ions

3.3.1. Simple separations demonstrated

In 1998 and 1999, the Guevremont group described the application of FAIMS as an ion filter for mass spectrometry [6,7,54]. The behavior of several positively charged small ions, including sodiated clusters with acetate, protonated methanol, and Cs^+ ions, were illustrated [54]. The possible applicability of ESI–FAIMS for small negative ions including bisulphate, acetate, and bicarbonate, and for large negative ions including substance P was investigated [54].

The potential for FAIMS to overcome limitations in mass spectrometry was illustrated with separations of isomers including leucine and isoleucine [45]. It was shown that the response to leucine was linear over more than two orders of magnitude (4 nM to 2.5 μM) and that a low concentration of leucine (4 nM) could be detected in the presence of a large (2.5 μM) excess of isoleucine.

Other examples of separations previously impossible by mass spectrometry alone, followed soon afterwards. These included a study of the separation of *o*-, *m*- and *p*-phthalic acids [38] using bath gases composed of mixtures of nitrogen and carbon dioxide. Although pure nitrogen or pure carbon dioxide could not separate all three isomers, a gas composition of about 5% carbon dioxide in nitrogen provided separation as well as a two- to seven-fold improvement in signal intensity. A similar separation of *o*-, *m*- and *p*-xylene [12] was later reported by the Eiceman group in New Mexico.

In an investigation of the possible application of ESI–FAIMS for the analysis of peptides, the Guevremont group studied the application of this new technology to the peptide leucine enkephaline (YGGFL) [55]. FAIMS was found to be capable of separating several types of leucine enkephaline based ions that are formed during the electrospray ionization process. Ions with similar *m*/*z* including $[M + H]^+$ and $[2M + 2H]^{2+}$ were separated, as were ions of a series of more complex species of the form $[2nM + nH]^{n+}$ all having *m*/*z* 1112. It was shown that these species become abundant during electrospray of solutions containing 10–100 μM leucine enkephalin. It was also shown that although such complexes are stable and can be separated into individual peaks in the CV spectrum of FAIMS, their identity is difficult to establish if the electric fields in the inlet of the mass spectrometer are sufficiently harsh to decompose the clusters to simpler species. Since peaks in the CV spectrum cannot easily be assigned without confirmation by mass spectrometry, the MS conditions for these measurements are critical to the correct identification of the ions.

In a more recent paper, the Eiceman group studied the field dependence of a series of protonated monomers and dimers of ketones [27]. The alpha function (Eq. (3)) of eight normal ketones with carbon numbers 3–10 (acetone to decanone) decreased monotonically from acetone through decanone. The proton bound dimers for each compound were formed under the same experimental conditions as the monomers, and the alpha functions for these ions were also determined. The alpha function for the proton bound dimer of acetone increased at low *E*/*N*, decreased beyond about 60 Td, and returned to near zero at 90 Td. A continuous decrease of the alpha function was observed for the proton bound dimer of decanone over the range of experimental *E*/*N*. The other proton bound dimers had intermediate behavior. The alpha function appears to change in a uniform, smooth manner amongst the set of compounds. Since the cross sections of the compounds studied here increase with the length of the carbon chain, their low-field mobility likely decreases from acetone through decanone. This would in turn result in decreasing the effective temperature (T_{eff}) for each compound from acetone to decanone when the comparison amongst these ions is made at a given field strength. This decreasing T_{eff} is expected to result in a decrease in the alpha function from acetone through decanone.

3.3.2. Small molecule applications related to the environment

This section will consider the application of FAIMS for measurements of small organic molecules of environmental interest. Inorganic ions of environmental interest were considered in Section 3.2, and the analysis of large organic compounds of environmental interest including microcystins will be considered in Section 3.4.

As part of a collaboration between the University of Alberta and the Guevremont group at NRC, the ESI–FAIMS–MS technology was applied to the analysis of trace level halogenated compounds produced during the disinfection of drinking water [56,57]. Haloacetic acids (HAA) are byproducts formed during chlorination, and are moni-

tored by water treatment facilities in the United States as part of the Stage 1 disinfectants/disinfection byproducts rule of the USEPA. The procedures used for this analysis are labor-intensive and time-consuming. The ESI–FAIMS–MS methods do not require extensive sample preparation, nor do they require any chromatography. In a recent report, the ESI–FAIMS–MS approach [58] was compared to EPA method 552.2 and standard method 6251 B used at city water utilities, and to a liquid-liquid extraction solid-phase microextraction (SPME) GC method applied at the Environmental Health Science Laboratory at the University of Alberta. The results from the ESI–FAIMS–MS method agreed well with the other methods, and had precision and accuracy comparable to GC methods.

The Eiceman group at New Mexico State University have described the detection of volatile compounds in ambient air inside and outside of buildings using a micromachined version of flat plate FAIMS [59]. Using a pair of small rectangular electrodes (about 20 mm × 30 mm) spaced apart by 1 mm, to which a 1 MHz waveform producing a peak field of about 12 kV/cm was applied, airborne contaminants attributed to the laboratory and to outside vehicular traffic on nearby highways were monitored continuously for up to 7 day periods. Ions were produced by photoionization, and detected amperometrically.

The Eiceman group also evaluated micromachined flat plate electrodes for field monitoring using GC–FAIMS [16]. The system permitted sensitive and specific detection of the insect pheromone Grandlure and a non-pheromone mixture they called Mix M. Detection limits measured for a series of evaluation compounds that included volatile aldehydes, ethers, esters and alcohols were 16–550 pg. Observed sensitivity was about 4 pA/ng.

In a further demonstration of the application of FAIMS to separations tandem with gas chromatography, the micromachined flat plate electrodes were used to identify sources of combustion using the fingerprint pattern of ions [60]. Vapor was sampled onto a solid-phase microextraction fiber, and analyzed using GC–MS and GC–FAIMS. Both techniques resulted in complex patterns that were suitable for identification of sources including combustion of cotton, paper, grass, and cigarette and engine exhaust. Reproducible characterization of the complex process (combustion) was obtained using simple sampling methods.

An ESI–FAIMS–MS system was used to demonstrate the identification and quantitation of naphthenic acids [61] that originate from crude oils. These compounds exhibit acute toxicity to aquatic species when discharged into tailing ponds as consequence of the oil sand extraction procedure. Mixtures of naphthenic acids from different sources were analyzed without extensive sample preparation [61]. A quantitative analysis of the mass and isomer distribution of naphenic acid components was obtained in 3 min. Separation of the complex mixture into simpler fractions using FAIMS permitted reliable elemental composition to be determined using high resolution MS, and further permitted structural information to be extracted from collision-induced dissociation experiments.

3.3.3. Small molecule applications related to the health sciences

This section will consider reports of separation and quantitative analysis of small organic compounds of biochemical interest. Section 3.4 will describe the application of FAIMS to larger peptides, to digests of proteins (proteomics) and to measurements of intact proteins.

The separation of leucine and isoleucine was demonstrated by Barnett et al. [45]. In a series of ESI–FAIMS–MS experiments using a triple quadrupole mass spectrometer, the negative ions of these isomeric amino acids were detected separately. It was shown that each isomer could be analyzed in the presence of over 600-fold excess of the other isomer. A signal-to-background improvement of over 50-fold was observed in the ESI–FAIMS–MS experiments in comparison with conventional ESI–MS with the same sample. Concentrations as low as 4 nM were detected.

The low background intensity observed using ESI–FAIMS–MS resulted in detection limits of 60 ng/mL for morphine and 20 ng/mL of codeine in urine samples [62]. This study included a quantitative analysis of NIST standard reference material 2381 (morphine and codeine in freeze dried urine). Ionization suppression was eliminated by a simple sample preparation using up to 200-fold dilution by methanol. Although the final concentrations of these compounds in the diluted samples were in the low pg/mL range, detection of morphine and codeine at ng/mL levels in the un-diluted urine was achieved.

A rapid quantitative method of analysis of amphetamine, methamphetamine, and some of their methylenedioxy derivatives using ESI–FAIMS–MS has been described by McCooeye et al. [63]. These compounds were extracted from urine using solid-phase microextraction and desorbed directly into a flow of solvent leading to an ESI source. Isotope dilution using deuterated (d_5) amphetamine was used for quantitative analysis. Detection limits in urine ranged from 0.2 ng/mL for 3,4-methylenedioxyethylamphetamine to 7.5 ng/mL for amphetamine. The authors reported that it was possible to obtain quantitative data within 20 min of arrival of the urine samples in the laboratory. On-site extraction using the SPME fiber is also feasible, eliminating the need to transport body fluids.

The capability of FAIMS to separate isobaric ions enabled the rapid quantitative isotope dilution analysis of diastereoisomers of ephedra alkaloids [64] in natural health products. A series of six ephedrine compounds was extracted from diet pills using pressurized fluid extraction and measured by a flow injection method requiring less than 3 min per sample. Quantitative measurements by FI–ESI–FAIMS–MS were compared to LC with UV detection. Good agreement was reported in a comparison of these methods. Some advantages of the FAIMS method included short analysis time, and a superior separation of the methylephedrine and methylpseu-

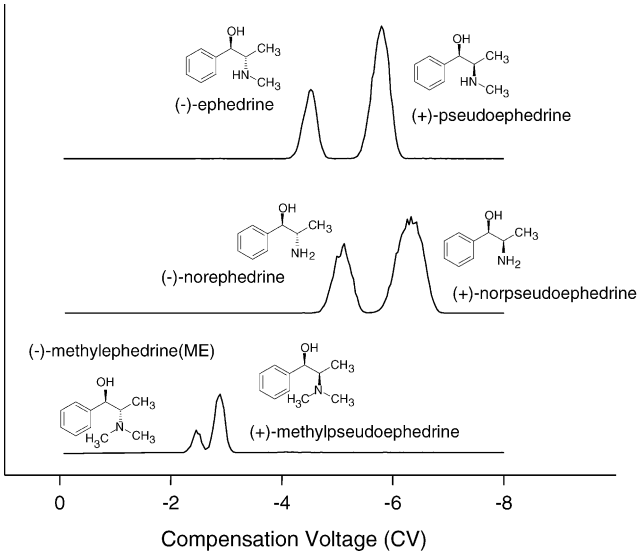

Fig. 6. FAIMS separation of the diastereoisomers of ephedrine alkaloids [64]. The compensation voltage was scanned while monitoring *m*/*z* 166 (ephedrine and pseudoephedrine), *m*/*z* 152 (norephedrine and norpseudoephedrine) and *m*/*z* 180 (methylephedrine and pseudomethylephedrine).

doephedrine pair of diastereoisomers relative to the LC–UV method. The FAIMS separation of these diastereoisomeric pairs is illustrated in Fig. 6.

Studies of the structure of carbohydrates and their conjugates by mass spectrometry are difficult because the ions resulting from biochemically important differences in structural details, such as the sequence of sugars, linkage type between sugars, and anomeric configurations, tend to be isobaric. Collision-induced dissociation of these ions also tend to produce daughter spectra which do not yield structurally informative ions. In a comprehensive report, Gabryelski and Froese [65] described an evaluation of FAIMS for the separation and identification of isomers of disaccharides. Although the separation of the anomers βDGlc(1–2)βDGalO$(CH_2)_8COOCH_3$ and αDGlc(1–2)βDGalO$(CH_2)_8COOCH_3$ as their Cs^+ adduct ions was incomplete (CV of 3.3 and 3.7 V, respectively), good separation (5.7 and 7.8 V) was achieved using the negative ion adducts of trichloroacetate. Good separation of Cl^- complexes of the linkage isomers βDGlc(1–3)βDGlcNHAcO-$(CH_2)_8COOCH_3$ and βDGlc(1–4)βDGlcNHAcO$(CH_2)_8$ $COOCH_3$ was reported. A number of successful separations of positional isomers having several amide groups were also reported. Preliminary results suggest that the FAIMS separation for this type of study is more effective using negative ions and that ion structure and the location of the charge site [65] are very important to the separation. The importance of gentle conditions in the entrance stages of the mass spectrometer was emphasized as it is important to avoid dissociation of the adduct ions into fragments which confound identification. Although FAIMS was observed to separate the labile complexes formed between the various disaccharides and certain halide and organohalide anions, considerable care was necessary to retain these adducts for correct MS identification.

3.3.4. Small molecule applications related to homeland security

Researchers at Mine Safety Appliances Company developed a cylindrical FAIMS [4] with electrometric detection for eventual military applications such as the portable detection of explosives, chemical warfare agents [66], and contraband materials [3]. Several patents [4,67–69] describe a gas chromatography–FAIMS system with a gas recycling system to enable field portability. A report from the National Institute of Justice [70] suggests that the MSA Instrument Division expected detection of explosives in the 10–1000 parts per trillion concentration range with this instrument.

In a series of papers between 2001 and 2004, Buryakov [13,14,28,30] evaluated the use of FAIMS for the detection of explosives and other chemical agents. A cylindrical version of FAIMS similar to that used by Guevremont [8] was adopted for the study of the explosive materials dinitrotoluene (DNT), trinitrotoluene (TNT), and pentaerythrite tetranitrate (PETN). The experimental conditions for optimal detection of these compounds were investigated. Consistent with the focusing properties of a cylindrical geometry FAIMS [8,9], the detected ion current increased with an increase of the applied waveform voltage [13]. A sensitivity decrease at the highest applied waveform voltage in this work was attributed to a non-linear increase in the coefficient of diffusion in strong fields [20]. Plots of the compensation fields for DNT, TNT and PETN suggest that the mobility of these compounds does not continue to show acceleration in the increase in mobility at high fields (data confirming this was reported later [30]), therefore the lower sensitivity at high fields (especially for PETN) is also a function of a decreasing focusing effect occurring when the ratio of mobility at high field to mobility at low field (during the waveform) passes a maximum value. The analytical response for DNT and TNT was not linear [13] but an analytical range for these compounds was reported to be 10^3. Detection limits estimated using a baseline electrometer current of 4×10^{-15} A, were 1×10^{-4} c_{sat} and 4.5×10^{-5} c_{sat} for the compounds with non-linear response (DNT and TNT) and a detection limit of 5×10^{-5} c_{sat} was measured directly for PETN. The c_{sat} is the concentration of saturated compound in air. This represents an excellent detection limit, since the concentration of TNT at room temperature is about 1 ppb [70].

Buryakov [30] studied the change in mobility of TNT, DNT, dinitrobenzene (DNB), trinitrobenzene (TNB), and dimethylphosphonate (DMMP) in strong fields. The FAIMS electrodes were modeled after the MSA design [4] and a customized waveform with a peak voltage of 2900 V (fields up to about 50 Td) was applied. Because the waveform used in this work was neither square nor the sum of two harmonics of the type used by Guevremont et al. [7], a method to extract the alpha coefficients that describe mobility in strong fields was developed specific to this waveform [2].

In a similar study, Buryakov [14] reported the change in mobility of TNT, DNT, DNB, TNB and mononitrotoluene (MNT) in fields exceeding 80 Td. As noted above, the rate of increase of mobility of these ions becomes constant between 40 and 60 Td, and further flattens beyond 60 Td. Presumably at higher fields, the mobility will begin to decrease (see type B ions [7]). Buryakov reports that the position of a peak on the compensation voltage spectrum is a function of the alpha function (Eq. (3) above), as well as experimental conditions (applied voltages, electrode spacing, gas pressure). The ratio of compensation voltages of an analyte and a reference compound was determined to be dependent on the ratios of their alpha functions [14], permitting qualitative identification when using an internal reference compound. This is valid when the series of α_2, α_4, α_6, ... are known for each compound, and these terms accurately reflect the change in mobility within the range of the experimentally applied fields. This does not suggest a constant ratio of compensation voltage of the analyte to the compensation voltage of the internal reference compound at all voltages of the applied waveform.

Buryakov [28] also described a combined GC–FAIMS system for the detection of a series of explosives, chemical warfare agents, and drugs. This multi-dimensional separation significantly enhances the likelihood of correct identification of the analyte, and minimizes the opportunity for interferences. Unfortunately, the peaks in the compensation voltage spectra (see Buryakov [28], Fig. 3) were not identified by mass spectrometry.

Eiceman et al. [18] recently described application of a miniature parallel plate FAIMS (referred to a differential mobility spectrometer) for the detection of the vapors of explosive materials. The study highlighted the potential advantages of using vapor-modified gas mixtures as carrier gases in FAIMS. Addition of 1000 ppm of methylene chloride was found to have the two-fold benefits; first an improvement of the atmospheric pressure chemistry of the ion source, and secondly this dopant caused significant shifts the compensation voltages of the analyte ions. Evaluation of a combined GC–FAIMS system for explosives was described, with detection of sub-nanograms of the explosives. Detection limits of the vapors of explosives provided in a continuous stream to the device (without MS detection) ranged from 0.08 to 8 ppb for TNT and 1,2-ethanediol, dinitrate, respectively (concentration of vapor determined using an exponential dilution system).

For comparison purposes, several commercial products are available for detection of explosive compounds. For example, a National Institute of Justice report available on the web [70] evaluates detection capabilities of several commercial systems, and indicates that the Graseby GVD4 detects explosive vapors at better than 1 part in 10^9 and the ION-SCAN 350 (and 400) from Smiths Detection (previously Barringer Instruments Inc.) was (at the time of the report) capable of detection of 50–200 pg of explosive materials. More recently a review of IMS products appeared in Analytical Chemistry [71], indicating that conventional benchtop and handheld IMS instruments have 0.1 ppb detection capability. It appears that FAIMS-based technology will equal, if not exceed, the performance of existing explosives detection products.

3.4. Separation and detection of medium and large organic ions

Early publications described the FAIMS separation of low mass ions derived from volatile compounds [2,3,7]. The first results with electrospray ionization combined with FAIMS (ESI–FAIMS) appeared in 1999 [8], where the separation of a series of amino acids was demonstrated. In a comprehensive overview, the combination of ESI and FAIMS was explored for a range of compounds, whose ions were transmitted in either positive or negative polarity of the dispersion voltage, and ranged in size from Cs^+ to substance P (negative ion, *m*/*z* 1347) [54]. Studies of the applicable concentration range of analyte suggested that the ESI formation of complex cluster ions of leucine enkephaline (*m*/*z* 556.5) may begin to take place at concentrations below 1 uM, and that the ESI formation of complexes at higher concentrations will limit the linear range for quantitative analysis [54,55]. Using FAIMS, the cluster ions are separated from the monomers and appear as separate peaks in the CV spectrum. The appearance of cluster ion peaks therefore results in a non-linear concentration response of the monomer peak. Although these clusters are not unique to FAIMS, and also form in a conventional ESI–MS experiment, the clusters usually dissociate in the MS interface to yield monomer ions, with the apparent linear response to analyte extended to higher concentration. The appearance of multiple analyte-related peaks in FAIMS is common [27,55,56], and all ion identification must utilize MS confirmation. This confirmation must be done at several conditions of MS interface voltages [55] to investigate whether CID in the interface of the mass spectrometer is yielding ions with simpler structure than the ions being transmitted through the FAIMS.

3.4.1. Large molecule applications related to the environment

Microcystins are a class of peptides that are formed by blooms of cyanobacteria (blue–green algae) in fresh and brackish waters. Some species release toxic compounds including the cyclic heptapeptide microcystin. Amino acid substitutions at two sites in the peptide result in as many as 50 different variants of microcystin. The combined ESI–FAIMS–MS system was used to evaluate qualitative and quantitative measurements of microcystin standard compounds (microcystin-LR, -RR and -YR) in water [72]. A comparison of measurements taken with ESI–MS and ESI–FAIMS–MS showed over 30-fold improvement in signal to background ratio (S/B) using FAIMS to detect a 66 nM sample of microcystin-YR. Detection limits were about 1–4 nM for the microcystin compounds tested. Detection limits are expected to be slightly degraded

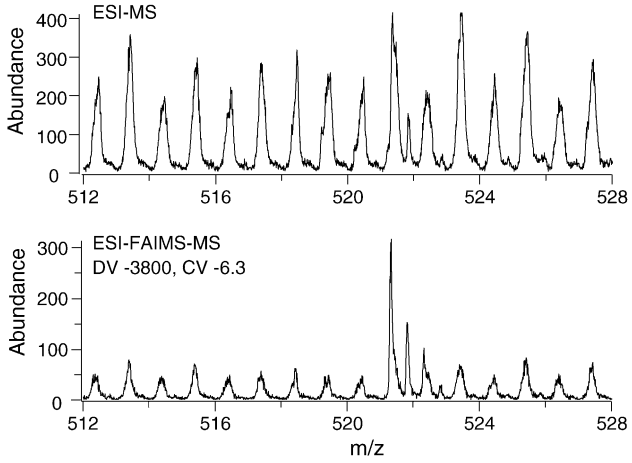

Fig. 7. ESI–MS and ESI–FAIMS–MS spectra of a tryptic digest of pig hemoglobin acquired with a Q-TOF instrument. The narrow mass range was selected to include the low abundance peptide MFLGFPTTK^{2+} (*m*/*z* 521.3).

when ESI–FAIMS–MS is applied to more complex samples [58,62].

3.4.2. Large molecule applications related to proteomics

The application of ESI–FAIMS–MS to studies of simple peptides [55] and to complex mixtures of peptides that result from the digestion of pure proteins [73–75] and to mixtures of proteins [75], have been reported.

The ESI–FAIMS–MS system was compared to conventional ESI–MS using a simple digest of pig hemoglobin [73]. The opportunity for improvement of S/B is illustrated in Fig. 7. It was also shown that single ion monitoring during a sweep of the CV may produce more than one peak. Mass spectra of these peaks indicated that isobaric peptides could be separated using FAIMS and be distinguished by their CV of transmission, thus increasing the opportunity to identify peptides. The CV of transmission of a number of known peptides from pig hemoglobin were tabulated, along with their *m*/*z* and ion cross sections reported in the literature [76]. Plots of CV against mass to charge ratio (*m*/*z*), mass of the molecule, charge of the peptide and collision cross section were shown. A correlation between CV and *m*/*z* was not observed for this limited set of compounds [73].

In a similar study using pig hemoglobin, the detection of peptides that were near or beyond the detection limit of conventional ESI–MS were investigated [74]. The MS/MS spectra of peptide ions collected with ESI–FAIMS–MS were compared to spectra collected without FAIMS. Since the FAIMS separation was shown to remove many background ions at the *m*/*z* of a peptide of interest, the MS/MS spectra collected using FAIMS contained a higher proportion of structurally informative ions than did the spectra collected with ESI–MS. The FAIMS assisted in detecting ions that fell below a S/B of 1 using conventional ESI–MS, and provided good quality MS/MS spectra for these low abundance ions.

In a more comprehensive investigation of the application of ESI–FAIMS–MS to the study of tryptic digests, Barnett et al. [75] reported results for individual digests, and mixtures of the digests of peptides from 13 proteins which included two variants of hemoglobin and five variants of albumin. Mixtures of carrier gases that included helium were found to improve the separation and sensitivity of detection of the peptide ions relative to results obtained with pure nitrogen. In addition, many additional peptide ions could be detected using a carrier gas composed of 1:1 He/N_2. A higher percentage He could not be added without increasing the likelihood of electrical discharge between the electrodes of FAIMS.

This study [75] also tabulated the CV of transmission of 38 singly, 208 doubly, and 36 triply charged peptide ions originating from the 13 proteins. A plot of the CV of the singly charged ions versus *m*/*z* showed a cluster centered near *m*/*z* 600 and CV of −10 V. This cluster lacked correlation between CV and *m*/*z*. Interestingly, the clusters generated for doubly and triply charged peptides were scattered within well-defined regions in the plot of CV versus *m*/*z*. For example, a great majority of the peptides having *m*/*z* between 500 and 1000 were found between CV −12 and −22 V. By comparison, the singly charged peptides of the same *m*/*z* range were all found between CV −7 and −12 V. Since the clusters of the doubly and triply charged ions were not significantly overlapped with the cluster from the singly charged ions, it was clear that FAIMS offered a new approach to reduce the number of singly charged ions observed in mass spectra of tryptic digests. This was illustrated in a comparison between ESI–MS and ESI–FAIMS–MS spectra collected using a mixture of the tryptic peptides of six proteins.

In recent reports, Thibault et al. [77,78] described the first comprehensive investigation of a nanoelectrospray LC–FAIMS–MS/MS system applied to proteomics. Using tryptic digests of several proteins, it was determined that the doubly charged peptide ions were preferentially transmitted through FAIMS from CV −15 to −22 and the more highly charged peptides transmitted above CV −20 V. Since each ion was typically transmitted over a range of CV of about 3 V (50% full width at half height), three CV voltages (−16, −18 and −21 V) were taken in steps of 1.5 s duration for LC–ESI–FAIMS–MS/MS experiments. A mixture of eight proteins (400 fmol each injection) was analyzed with and without FAIMS. This comparison showed that combined FAIMS nano LC–MS analysis yielded approximately 17% more multiply charged ions accompanied by a decrease in the singly charged ions, compared to a conventional nanoelectrospray analysis. Since the background of ions was reduced using FAIMS, an additional benefit of simplification of the peptide sequencing using MS/MS spectra was reported. A 10-fold gain in signal-to-noise compared to conventional nano LC–MS was observed with detection limits ranging from high attomoles to low femtomoles for protein digests. This work was carried out using a Waters Q-TOF micro equipped with a CapLC liquid chromatograph, Waters C_{18} symmetry precolumn and 10 cm × 150 μm i.d. Jupiter

5 μm C_{18} analytical column. Peptide elution was achieved using linear gradient of 10–60% acetonitrile (0.2% formic acid) in 60 min.

3.4.3. ESI–FAIMS–MS studies of intact proteins

The development of ESI has enabled the study of the ions of intact proteins in the gas-phase, absent the solvent interactions typical of condensed phase. The +5 to +13 charge states of bovine ubiquitin were generated using ESI, and these ions passed through FAIMS [79]. The large size of these ions, and the theory described by Mason and McDaniel [20] suggested that the mobility of an intact protein ion at high fields might not be appreciably different than its mobility at low fields. Interestingly, it was observed via single ion monitoring of the *m*/*z* of each of the multiply charged ions of bovine ubiquitin, that these ions passed through FAIMS at non-zero values of CV [79]. Moreover, in some cases, two or three peaks were observed during this CV scan [79]. Further investigation of these multiplets in the CV spectrum, was performed by varying sample solution pH, using samples with denaturing solution conditions, varying solvent compositions, and using additions of species including salts. The results of these measurements led the authors to conclude that the ions separated by FAIMS were intact protein ions differing from each other either in some aspect of three-dimensional conformation and/or in the charge distribution within the ion that may control the ability of the ion to change structure in response to the electric field strength. The existence of multiple sub-species of intact ubiquitin ions is consistent with prior literature in which collisions between the protein ion and bath gas molecules using triple quadrupole MS and conventional drift tube ion mobility spectrometer systems have been used to elucidate certain aspects of the properties of the ions. For example, the drift velocity of some sub-species of the +7 to +10 ions of bovine ubiquitin were shown to differ from each other, and this drift velocity was used to calculate the cross sections of the ions [80]. Similarly, hydrogen/deuterium (H/D) exchange rates of the sub-species of the bovine ubiquitin [81,82] ion can be attributed to the availability of sites for exchange, and thus reflect the degree of folding of the protein ion. The specific property of the ion that is reflected by FAIMS data is presently unknown. Nevertheless, for convenience in this report, these sub-species will be called ‘conformers’.

The cross sections of the intact ions of bovine ubiquitin were measured [83,84] in a triple quadrupole mass spectrometer using an energy loss technique pioneered by Douglas et al. [85,86]. In the ESI–MS/MS system used by Douglas et al., the cross section of a protein ion was estimated by selecting the ion in Q1, decreasing its kinetic energy via collisions with a bath gas in Q2, and by measuring the residual kinetic energy of the ion through its ability to overcome a stopping potential applied to Q3 (or a comparable ion lens). This method is not applicable if two or more sub-species of differing cross section coexist at a given *m*/*z*. However, the method becomes much more widely applicable if the species are separated by FAIMS prior to introduction to the instrument. Purves et al. [83] determined the cross sections of 19 uniquely separated species corresponding to ions of +5 to +13 charge states of bovine ubiquitin. In a second report [84], species of the charge states +11 to +15 of bovine ubiquitin were studied.

The cross sections measured using the FAIMS–energy loss experiment [83] agreed well with cross sections determined using conventional drift tube ion mobility spectrometry [80]. This interesting result suggests that only a small number of conformers are generated in the electrospray ionization of bovine ubiquitin and that, although the FAIMS and drift tube mobility experiments sample uniquely different properties of the ions, the presence of small numbers of coexisting species is observed in both experiments. The energy loss experiment then confirmed that FAIMS had indeed separated species that appear to be the same species in the drift tube ion mobility separation. Furthermore, it was shown that FAIMS separated two ions of +12 charge state that were not separated by drift tube ion mobility. The existence of these two species was previously established using hydrogen/deuterium (H/D) exchange [81,82].

The doubly charged $[M + 2H]^{2+}$ ion of bradykinin was studied using a combination of ESI–FAIMS–MS, hydrogen/deuterium exchange and energy loss measurements [87]. Deuterated water vapor was added to the FAIMS carrier gas, and exchange reactions took place inside the FAIMS analyzer during the approximately 150 ms required for the ion to pass through FAIMS. The exchange of hydrogen by deuterium on the bradykinin ion yielded an envelope of isotopomers whose average *m*/*z* exceeded that of the original ion. It was observed that the ion species transmitted through FAIMS at a CV of approximately 6.3 V was actually two species whose isotopomer distributions were centered near *m*/*z* 532 and 535. Evaluation of the data from both H/D and FAIMS indicated the presence of four distinct species of the $[M + 2H]^{2+}$ ion of bradykinin, whose cross sections were reported. Taken alone, neither FAIMS, nor the H/D exchange experiments are capable of detecting the presence of all four conformers, and only through combined data from both methods was the presence of these conformers deduced.

The studies of the conformers of bovine ubiquitin and bradykinin demonstrated that FAIMS is sensitive to the three-dimensional structure of the protein ion. Five cytochrome c protein variants: dog, horse, sheep, cow and rat; were studied to determine whether subtle changes in the amino acid sequence in a particular protein would result in changes in the CV spectra collected using FAIMS [88]. The number of conformers of cytochrome c exceeded that of bovine ubiquitin, and sweeps of CV taken while monitoring the *m*/*z* of the +17 and +18 charge states yielded a series of complex fingerprint patterns of the coexisting conformers within each charge state. The patterns of peak CV values and the relative abundance of coexisting conformers of each charge state within the series of protein variants were compared. In every case, where the amino acid sequence of the protein was altered, a change in the pattern of the conformers of one or more charge states was detected [88]. Two variants of cytochrome

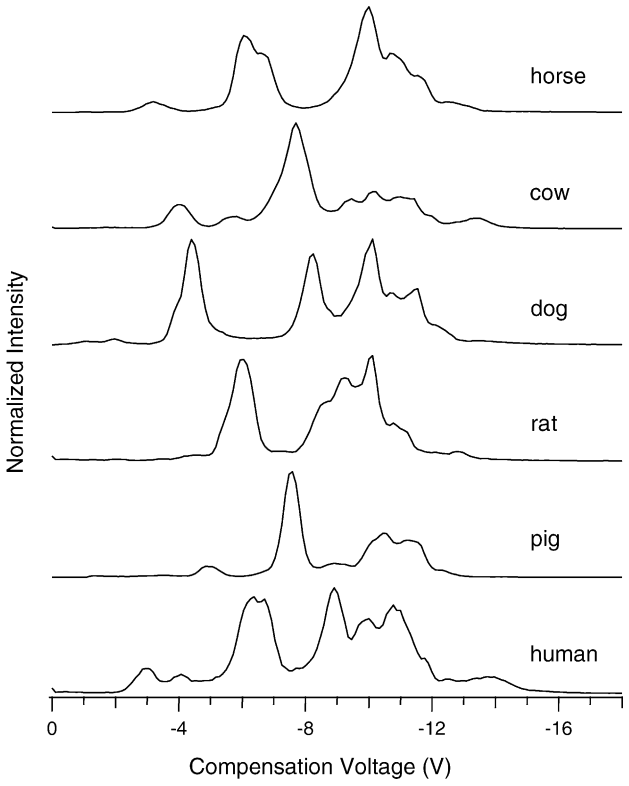

Fig. 8. The CV spectra for the +18 charge state (alpha chain) of six hemoglobin variants; horse (m/z = 840.7), cow (m/z = 837.3), dog (m/z = 846.4), rat (m/z = 845.3), pig (m/z = 836.5), and human (m/z = 841.3). The spectra were acquired using six separate solutions each containing a particular variant.

c originating from cow and sheep have identical amino acid sequences, and could not be distinguished from each other by these experiments.

Fig. 8 illustrates scans of compensation voltage while monitoring the m/z of the +18 charge state of the alpha chain of hemoglobin originating from several species [89]. The pattern of conformers appears to reflect differences in the structures and relative abundances of the conformers originating from variants of the protein. The ESI–FAIMS–MS technology appears to provide a potential tool for the rapid screening of proteins to identify cases of anomalous amino acid sequence. It remains to be determined if the differences in conformation detected by FAIMS offer insight into the relationship between the folding of proteins and disease.

Recently Ashcroft et al. [90] described FAIMS separation of the conformers of several multiply-charged ions of β_2-microglobulin, in a series of experiments designed to evaluate possible application of FAIMS to the study of protein folding, with a longer term objective of obtaining insight into the roles that protein conformers may play in disease. Several conformers of the amyloidogenic protein β_2-microglobulin were separated using ESI–FAIMS–MS under chemical conditions ranging from pH 2.0 to 6.0, which resulted in varying degrees of denaturation of the multiply charged ions of the protein. Species separated by FAIMS were associated with folded, partly folded and acid unfolded versions of the protein. For a comparison, a single amino acid mutant of β_2-microglobulin was also analyzed under the same ESI–FAIMS–MS conditions. Since this mutant is destabilized relative to the wild-type protein, the mutant undergoes acid denaturation at pH higher than those required by the wild-type. From these experiments, it was concluded that FAIMS showed a remarkable ability to separate conformers that are co-populated in solution, a feat not currently achievable by any other biophysical techniques.

4. Future development of FAIMS

The FAIMS technology has introduced several new opportunities into the field of chemical analysis using mass spectrometry. It is the exploration and exploitation of these key features that characterize the future of FAIMS.

FAIMS separates ions on the basis of the properties of the interactions/collisions between the ion and the bath gas molecules, a property that has not previously been exploited either in DTIMS or in any form of MS/MS. The separation is a function of the structural properties of the ion and the bath gas(es). It is also known that the formation of analyte ion adducts may result in new labile species that can be separated by FAIMS. The opportunity of exploiting this multifaceted field is significant.

Since adducts can have significant impact on the separation of ions in FAIMS, the FAIMS device also has the capability to detect non-ionic species indirectly through their effect on the behavior of ions. For example, a stream of monitor ions can be produced and continuously transmitted through FAIMS by a carrier gas. A non-ionizable target analyte is added to the carrier gas. The presence of this target analyte, when it interacts with the monitor ion, is detected by a shift in the CV of the monitor ion.

The FAIMS technology is capable of focusing and trapping ions at atmospheric pressure. This capability has been sought after since the advent of ion trapping systems that function at the low pressures of a mass spectrometer. Ion trapping in FAIMS devices may be the future basis for improving the sensitivity of mass spectrometers, and for improving the ability of a mass spectrometer to simultaneously process ions from several parallel experiments.

The FAIMS separation technology can be and will be applied to various types of atmospheric pressure ion sources, as well as to sources operating above and below atmospheric pressure. Preliminary results with atmospheric pressure MALDI have been reported, and further work is expected to widen the range of ion sources for which FAIMS is available.

5. Conclusions

FAIMS is a new technology that offers significant promise for extending the capability of mass spectrometry to solve problems in chemical analysis.

FAIMS is a technology that is physically located between the atmospheric pressure ion source and the mass spectrometer. Since FAIMS does not displace any existing technology, all pre-ionization sample-handling and chromatographic separations remain viable, as do all post-FAIMS ion-processing technology, including the full capabilities of a wide range of types of mass spectrometers. FAIMS separates ions continuously in a flowing stream, and is therefore fully compatible with all types of mass spectrometers.

It has been demonstrated that several types of isobaric ions can be separated by FAIMS, ranging from the positional isomers of small molecules, to the conformers of intact proteins. The FAIMS separation is fast, and may therefore replace slower separations previously used to solve these problems.

Signal-to-background ratios (S/B) can be improved by passing ions originating from atmospheric pressure sources such as ESI and MALDI through FAIMS to select the ion of interest in preference to the background ions. This separation takes place prior to the MS experiment, thus all of the MS features remain operable without limitations. The improvement of S/B arising from the removal of background ions leads to an improvement in detection limits, which in some cases will allow simplification of sample handling via preconcentration and/or extraction. Reduction of sample handling, and reduction of the requirements for time-consuming condensed phase separations translate into improved cost-efficiency of chemical analysis.

FAIMS offers separations that simplify complex mixtures. This separation is orthogonal to existing chromatography, as well as to *m*/*z* separation in the mass spectrometer. Hybrid combinations of LC–FAIMS–MS offer significant future opportunities for the analysis of very complex mixtures. Hybrid combinations of FAIMS–MS with other gas-phase separations including DTIMS are also likely to be successful when applied to complex mixtures.

References

[1] M.P. Gorshkov, USSR Inventors Certificate No. 966583 (1982).
[2] I.A. Buryakov, E.V. Krylov, E.G. Nazarov, U.K. Rasulev, Int. J. Mass Spectrom. Ion Processes 128 (1993) 143.
[3] B. Carnahan, S. Day, V. Kouznetsov, M. Matyjaszczyk, A. Tarassov, Proceedings of the 41st Annual ISA Analysis Division Symposium, Framingham, MA, 21–24 April, 1996.
[4] B.L. Carnahan, A.S. Tarassov, US Patent 5,420,424 (1995).
[5] V. Kouznetsov, US Patent 5,801,379 (1998).
[6] R.W. Purves, R. Guevremont, S. Day, M. Matyjaszczyk, C.W. Pipich, Proceedings of the 46th ASMS Conference on Mass Spectrometry and Allied Topics, Orlando, FL, 31 May–4 June, 1998.
[7] R.W. Purves, R. Guevremont, S. Day, C.W. Pipich, M.S. Matyjaszczyk, Rev. Sci. Instrum. 69 (1998) 4094.
[8] R. Guevremont, R.W. Purves, Rev. Sci. Instrum. 70 (1999) 1370.
[9] E.V. Krylov, Tech. Phys. 44 (1999) 113.
[10] R. Guevremont, R.W. Purves, D.A. Barnett, L. Ding, Int J. Mass Spectrom. 193 (1999) 45.
[11] G.A. Eiceman, E.G. Nazarov, R.A. Miller, Proceedings of the 48th ASMS Conference on Mass Spectrometry and Allied Topics, 10–15 June, 2000.
[12] R.A. Miller, E.G. Nazarov, G.A. Eiceman, A.T. King, Sens. Actuators A 91 (2001) 307.
[13] I.A. Buryakov, Y.N. Kolomiets, B.V. Luppu, J. Anal. Chem. 56 (2001) 336.
[14] I.A. Buryakov, Talanta 61 (2003) 369.
[15] G.E. Spangler, Field Anal. Chem. Technol. 4 (2000) 255.
[16] G.A. Eiceman, B. Tadjikov, E. Krylov, E.G. Nazarov, R.A. Miller, J. Westbrook, P. Funk, J. Chromatogr. A 917 (2001) 205.
[17] C.A. Veasey, C.L.P. Thomas, Analyst 129 (2004) 198.
[18] G.A. Eiceman, E. Krylov, N. Krylova, E.G. Nazarov, R.A. Miller, Anal. Chem., in press.
[19] G.A. Eiceman, Z. Karpas, Ion Mobility Spectrometry, CRC Press, Boca Raton, FL, 1994.
[20] E.A. Mason, E.W. McDaniel, Transport Properties of Ions in Gases, Wiley, New York, 1988.
[21] H.W. Ellis, R.Y. Pai, E.W. McDaniel, E.A. Mason, L.A. Viehland, At. Data Nucl. Data Tables 17 (1976) 177.
[22] H.W. Ellis, E.W. McDaniel, D.L. Albritton, L.A. Viehland, S.L. Lin, E.A. Mason, At. Data Nucl. Data Tables 22 (1978) 179.
[23] H.W. Ellis, M.G. Thackston, E.W. McDaniel, E.A. Mason, At. Data Nucl. Data Tables 31 (1984) 113.
[24] L.A. Viehland, E.A. Mason, At. Data Nucl. Data Tables 60 (1995) 37.
[25] R.A. Miller, G.A. Eiceman, E.G. Nazarov, A.T. King, Sens. Actuators B 67 (2000) 300.
[26] E. Krylov, Instrum. Exp. Tech. 40 (1997) 628.
[27] E. Krylov, E.G. Nazarov, R.A. Miller, B. Tadjikov, G.A. Eiceman, J. Phys. Chem. A 106 (2002) 5437.
[28] I.A. Buryakov, J. Chromatogr. B 800 (2004) 75.
[29] R. Guevremont, D.A. Barnett, R.W. Purves, L.A. Viehland, J. Chem. Phys. 114 (2001) 10270.
[30] I.A. Buryakov, Tech. Phys. 47 (2002) 1453.
[31] L.A. Viehland, R. Guevremont, R.W. Purves, D.A. Barnett, Int. J. Mass Spectrom. 197 (2000) 123.
[32] R. Guevremont, L. Ding, B. Ells, D.A. Barnett, R.W. Purves, J. Am. Soc. Mass Spectrom. 12 (2001) 1320.
[33] R. Guevremont, L. Ding, R.W. Purves, D.A. Barnett, Proceedings of the 50th ASMS Conference on Mass Spectrometry and Allied Topics, Orlando, FL, 2–6 June, 2002.
[34] R. Guevremont, D.A. Barnett, B. Ells, R.W. Purves, G.U. Thekkadath, L.A. Viehland, Proceedings of the 51st ASMS Conference on Mass Spectrometry and Allied Topics, Montreal, Canada, 8–12 June, 2003.
[35] A. Shvartsburg, K. Tang, R.D. Smith, J. Am. Soc. Mass Spectrom., in press.
[36] D.A. Barnett, B. Ells, R. Guevremont, R.W. Purves, L.A. Viehland, J. Am. Soc. Mass Spectrom. 11 (2000) 1125.
[37] K. Iinuma, E.A. Mason, L.A. Viehland, Mol. Phys. 61 (1987) 1131.
[38] D.A. Barnett, R.W. Purves, B. Ells, R. Guevremont, J. Mass Spectrom. 35 (2000) 976.
[39] L.C. Rorrer III, R. Guevremont, D.A. Barnett, R.A. Yost, Proceedings of the 50th ASMS Conference on Mass Spectrometry and Allied Topics, Orlando, FL, June 2–6, 2002.
[40] N. Krylova, E. Krylov, G.A. Eiceman, J.A. Stone, J. Phys. Chem. A 107 (2003) 3648.
[41] A. Shvartsburg, K. Tang, R.D. Smith, Anal. Chem., submitted for publication.
[42] R. Guevremont, http://www.faims.com/.
[43] G.E. Spangler, R.A. Miller, Int. J. Mass Spectrom. 214 (2002) 95.
[44] D.A. Barnett, R.W. Purves, R. Guevremont, Nucl. Instrum. Methods A 450 (2000) 179.
[45] D.A. Barnett, B. Ells, R.W. Purves, R. Guevremont, J. Am. Soc. Mass Spectrom. 10 (1999) 1279.
[46] E. Krylov, Int. J. Mass Spectrom. 225 (2003) 39.

[47] B.L. Sharp, A.B. Sulaiman, K.A. Taylor, B.N. Green, J. Anal. At. Spectrom. 12 (1997) 603.
[48] D.A. Barnett, R.W. Purves, R. Guevremont, Appl. Spectrosc. 53 (1999) 1367.
[49] R. Handy, D.A. Barnett, R.W. Purves, G. Horlick, R. Guevremont, J. Anal. At. Spectrom. 15 (2000) 907.
[50] B. Ells, D.A. Barnett, R.W. Purves, R. Guevremont, J. Environ. Monit. 2 (2000) 393.
[51] C. Meng, L. Ding, Z. Mester, Anal. Chem. 75 (2003) 5847.
[52] C.J. Smith, I.D. Wilson, F. Abou-Shakra, R. Payne, T.C. Parry, P. Sinclair, D.W. Roberts, Anal. Chem. 75 (2003) 1463.
[53] S. McSheehy, Z. Mester, J. Anal. Atom. Spectrom. 19 (2004) 373.
[54] R.W. Purves, R. Guevremont, Anal. Chem. 71 (1999) 2346.
[55] R. Guevremont, R.W. Purves, J. Am. Soc. Mass Spectrom. 10 (1999) 492.
[56] B. Ells, D.A. Barnett, K. Froese, R.W. Purves, S. Hrudey, R. Guevremont, Anal. Chem. 71 (1999) 4747.
[57] B. Ells, D.A. Barnett, R.W. Purves, R. Guevremont, Anal. Chem. 72 (2000) 4555.
[58] W. Gabryelski, F. Wu, K.L. Froese, Anal. Chem. 75 (2003) 2478.
[59] G.A. Eiceman, E.G. Nazarov, B. Tadjikov, R.A. Miller, Field Anal. Chem. Tech. 4 (2000) 297.
[60] G.A. Eiceman, A. Tarrasov, P.A. Funk, S.E. Hughs, E.G. Nazarov, R.A. Miller, J. Sep. Sci. 26 (2003) 285.
[61] W. Gabryelski, K.L. Froese, Anal. Chem. 75 (2003) 4612.
[62] M.A. McCooeye, B. Ells, D.A. Barnett, R.W. Purves, R. Guevremont, J. Anal. Toxicol. 25 (2001) 81.
[63] M.A. McCooeye, Z. Mester, B. Ells, D.A. Barnett, R.W. Purves, R. Guevremont, Anal. Chem. 74 (2002) 3071.
[64] M.A. McCooeye, L. Ding, G.J. Gardner, C.A. Fraser, J. Lam, R.E. Sturgeon, Z. Mester, Anal. Chem. 75 (2003) 2538.
[65] W. Gabryelski, K.L. Froese, J. Am. Soc. Mass Spectrom. 14 (2003) 265.
[66] D.E. Riegner, C.S. Harden, B. Carnahan, S. Day, Proceedings of the 45th ASMS Conference on Mass Spectrometry and Allied Topics, Palm Springs, CA, 1–5 June, 1997.
[67] B.L. Carnahan, A.S. Tarassov, US Patent 5,723,861 (1998).
[68] J.M.A. Pertinarides, A.S. Tarassov, B.L. Carnahan, C.W. Pipich, V. Kouznetsov, US Patent 5,763,876 (1998).
[69] R.E. Uber, V. Kouznetsov, A.S. Tarassov, B.L. Carnahan, C.W. Pipich, US Patent 5,736,739 (1998).
[70] C.L. Rhykerd, D.W. Murray, D.W. Hannum, J.E. Parmeter, http://www.ncjrs.org/pdffiles1/nij/178913-1.pdf and http://www.ncjrs.org/pdffiles1/nij/178913-2.pdf (1999).
[71] K. Cottingham, Anal. Chem. 75 (2003) 435A.
[72] B. Ells, K. Froese, S.E. Hrudey, R.W. Purves, R. Guevremont, D.A. Barnett, Rapid Commun. Mass Spectrom. 14 (2000) 1538.
[73] R. Guevremont, D.A. Barnett, R.W. Purves, J. Vandermey, Anal. Chem. 72 (2000) 4577.
[74] D.A. Barnett, L. Ding, B. Ells, R.W. Purves, R. Guevremont, Rapid Commun. Mass Spectrom. 16 (2002) 676.
[75] D.A. Barnett, B. Ells, R. Guevremont, R.W. Purves, J. Am. Soc. Mass Spectrom. 13 (2002) 1282.
[76] S.J. Valentine, A.E. Counterman, D.E. Clemmer, J. Am. Soc. Mass Spectom. 10 (1999) 1188.
[77] K. Venne, E. Bonneil, K. Eng, D.A. Barnett, P. Thibault, Proceedings of the 51st ASMS Conference on Mass Spectrometry and Allied Topics, Montreal, PQ, 8–12 June, 2003.
[78] K. Venne, E. Bonneil, K. Eng, P. Thibault, Pharmagenomics 4 (2004).
[79] R.W. Purves, R. Guevremont, D. Barnett, Int. J. Mass Spectrom. 197 (2000) 163.
[80] J.W. Li, J.A. Taraszka, A.E. Counterman, D.E. Clemmer, Int. J. Mass Spectrom. 187 (1999) 37.
[81] C.J. Cassady, S.R. Carr, J. Mass Spectrom. 31 (1996) 247.
[82] M.A. Freitas, C.L. Hendrickson, M.R. Emmett, A.G. Marshall, Int. J. Mass Spectrom. 187 (1999) 565.
[83] R.W. Purves, D.A. Barnett, B. Ells, R. Guevremont, J. Am. Soc. Mass Spectrom. 11 (2000) 738.
[84] R.W. Purves, D.A. Barnett, B. Ells, R. Guevremont, J. Am. Soc. Mass Spectrom. 12 (2001) 894.
[85] D.J. Douglas, J. Am. Soc. Mass Spectrom. 5 (1994) 17.
[86] T. Covey, D.J. Douglas, J. Am. Soc. Mass Spectrom. 4 (1993) 616.
[87] R.W. Purves, D.A. Barnett, B. Ells, R. Guevremont, Rapid Commun. Mass Spectrom. 15 (2001) 1453.
[88] R. Guevremont, R.W. Purves, PCT Publication WO 03/067261 (2003).
[89] R.W. Purves, L. Ding, B. Ells, R. Guevremont, D.A. Barnett, Proceedings of the 50th ASMS Conference on Mass Spectrometry and Allied Topics, Orlando, FL, 2–6 June, 2002.
[90] A.J.H. Borysik, P. Read, D.R. Little, R.H. Bateman, S.E. Radford, A.E. Ashcroft, Rapid Commun. Mass Spectrom. 18 (2004) 2229.